Lacunarity analysis: A general technique for the analysis of spatial patterns

Roy E. Plotnick
Department of Geological Sciences, University of Illinois at Chicago, 845 West Taylor Street, Chicago, Illinois 60607-7059

Robert H. Gardner
University of Maryland, Appalachian Environmental Laboratory, Frostburg, Maryland 21532

William W. Hargrove
Environmental Sciences Division, Oak Ridge National Laboratory, Oak Ridge, Tennessee 37831-6038

Karen Prestegaard
Department of Geology, University of Maryland, College Park, Maryland 20742

Martin Perlmutter
Energy Systems Division, Argonne National Laboratory, 9700 South Cass Avenue, Argonne, Illinois 60439
(Received 21 April 1995; revised manuscript received 14 December 1995)

Lacunarity analysis is a multiscaled method for describing patterns of spatial dispersion. It can be used with both binary and quantitative data in one, two, and three dimensions. Although originally developed for fractal objects, the method is more general and can be readily used to describe nonfractal and multifractal patterns. Lacunarity analysis is broadly applicable to many data sets used in the natural sciences; we illustrate its application to both geological and ecological data. [S1063-651X(96)01505-X]

PACS number(s): 07.05.Kf, 89.60.+x, 91.65.−n, 92.40.Fb

I. INTRODUCTION

An important goal in the natural sciences, such as geology, ecology, and epidemiology, is the quantification of spatial patterns. However, these patterns are often complex, exhibit scale-dependent changes in structure, and are correspondingly difficult to identify and describe. As a result, the advent of fractal mathematics has been greeted enthusiastically by many natural scientists and fractal techniques have been increasingly applied (Barton and La Pointe [1]). To date, however, this application has been generally restricted to the calculation of the fractal dimension and related parameters. Newer methods, such as multifractals, are only beginning to be used (Milne [2], Lam and De Cola [3]).

In this paper we will show how the concept of lacunarity, which was originally developed to describe a property of fractals (Mandelbrot [4]; Lin and Yang [5]; Gefen, Meir, and Aharony [6]; Allain and Cloitre [7]), can be extended to the description of spatial distribution of real data sets, including, but not restricted to, those with fractal and multifractal distributions.

The approach we use is an elaboration of the lacunarity algorithm developed by Allain and Cloitre [7], which was introduced to ecologists in a previous paper [8]. In this paper the algorithm is used as the basis of a more general approach to the study of spatial distributions. We review the algorithm and show how it can be used to describe both binary and count (quantitative) data and can be applied to data of any dimensionality. The method is applied to a number of model data sets, including multifractals, and we demonstrate how it can be used to uncover scale-dependent changes of spatial structure. We then document the application of the method to empirical data sets from ecology and geology.

II. THE GLIDING BOX ALGORITHM AND LACUNARITY ANALYSIS

A. The gliding box algorithm: Applications to binary sets

As defined by Gefen, Meir, and Aharony [6], lacunarity is the deviation of a fractal from translational invariance. Translational invariance can, of course, also be a property of nonfractal sets [7]. In addition, translational invariance is highly scale dependent; sets which are heterogeneous at small scales can be quite homogeneous when examined at larger scales or vice versa. Lacunarity can thus be considered a scale-dependent measure of heterogeneity or texture of an object, whether or not it is fractal [7].

A number of algorithms have been proposed for measuring this property [5,6]; we have adopted the intuitively clear and computationally simple ''gliding box'' method of Allain and Cloitre [7]. Simple examples demonstrate the use of this algorithm for binary data. Illustrated in Fig. 1 are five one-dimensional sets which differ in translational invariance; they could, for example, represent such empirical data as the occurrence of a tree species along a transect. All sets have the same length ($M=256$) and the same number of occupied sites ($S=44$). Set A's points are all clustered at the extremes of the line; set B's approximate a fractal Lévy dust; set C's are randomly placed; and set D's are regularly distributed. In set E, the points occur in clumps of four points but these clumps are randomly distributed. Set E could represent a case where groups of trees (the clumps) are themselves randomly spaced; i.e., there are two distinct scales to the pattern.

A box of length r is placed at the origin of one of the sets (Fig. 1). The number of occupied sites within the box (box mass equal to s) is now determined. The box is moved one

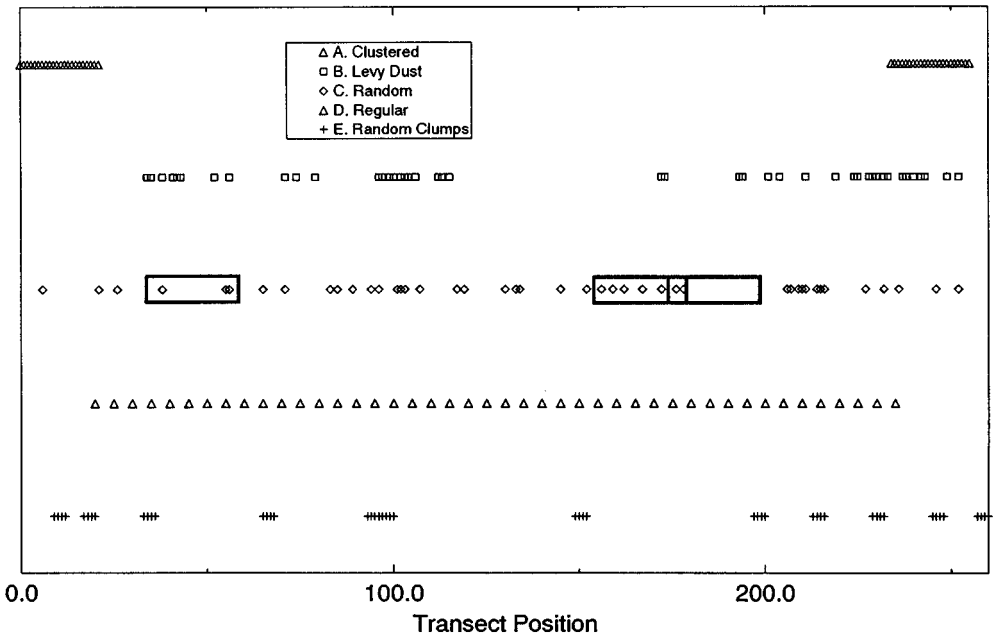

FIG. 1. Five one-dimensional sets containing the same number of points but differing in spatial distribution. The abscissa units are arbitrary. The boxes on set C represent three positions of a gliding box of length 9. Redrawn from Plotnick [14].

space along the set and the box mass is again counted. This process is repeated over the entire set, producing a frequency distribution of the box masses $n(s,r)$. This frequency distribution is converted into a probability distribution $Q(s,r)$ by dividing by the total number of boxes $N(r)$ of size r. The first and second moments of this distribution are now determined:

$$Z(1)=\Sigma sQ(s,r), \tag{1}$$

$$Z(2)=\Sigma s^2Q(s,r). \tag{2}$$

The lacunarity for this box size is now defined as

$$\Lambda(r)=Z(2)/[Z(1)]^2. \tag{3}$$

This calculation is repeated over a range of box sizes, ranging from $r=1$ to some fraction of M (we usually use $M/2$). A log-log plot of the lacunarity versus the size of the gliding box is then produced. Lacunarity plots for the sets in Fig. 1 are illustrated in Fig. 2.

The statistical behavior of $\Lambda(r)$ and the shape of the lacunarity curves can best be understood by recalling that

$$Z(1)=\overline{s(r)}, \tag{4}$$

$$Z(2)=s_s^2(r)+\overline{s^2}(r), \tag{5}$$

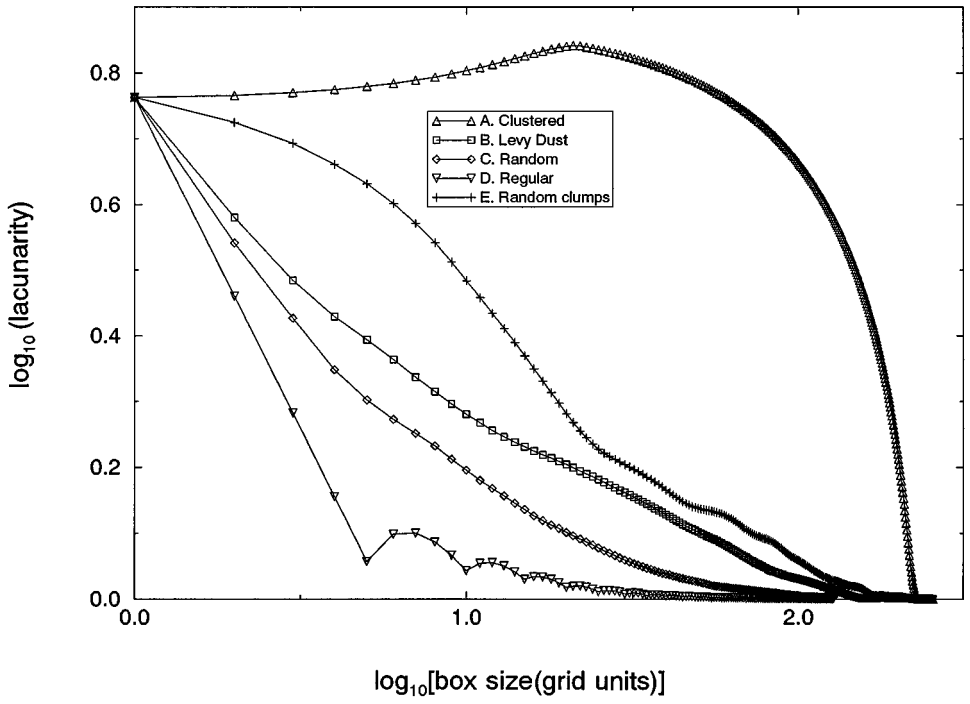

FIG. 2. Lacunarity analyses for the distributions shown in Fig. 1. Lacunarity is dimensionless. Redrawn from Plotnick [14].

where $\overline{s(r)}$ is the mean and $s_s^2(r)$ the variance of the number of sites per box. As a result,

$$\Lambda(r) = s_s^2(r)/\overline{s^2}(r) + 1. \quad (6)$$

The lacunarity statistic is thus a dimensionless representation of the variance to mean ratio and is closely related, therefore, to a number of statistics, such as Morisita's index, that have long been used in ecology [9].

From this relationship, and by examining the lacunarity curves in Fig. 2, it can be shown that the lacunarity for binary data is a function of the following.

(1) The fraction $P(=S/M)$ of sites that are occupied. As the mean number of occupied sites $Z(1)$ goes to zero, Λ goes to ∞. Sparse sets will thus have higher lacunarities than dense sets, for the same gliding box sizes.

(2) The size r of the gliding box. In general, except for highly clustered sets (e.g., set A in Fig. 1) larger boxes will be more translationally invariant than smaller boxes; i.e., the second moment declines relative to the first. The same set will thus have lower lacunarities as the size of the boxes increases. For all sets, since $Q(1,1)=P$, $Z(2)/[Z(1)]^2 = P/P^2$, and $\Lambda(1)=1/P$. This value is solely a function of the percentage of occupied sites and is independent of the overall size of the set and details of its geometry. A similar constraint occurs if the box is the size of the entire set; then the variance component of the second moment is 0 and $\Lambda(M)$ must equal 1. As a result, since all five sets in Fig. 1 have the same values of P and M, the y and x intercepts of their lacunarity curves are identical.

(3) The geometry of the set. For a given P and r higher lacunarity indicates greater clumping. Set A in Fig. 1 is highly clustered, with a single large gap in the middle. For all $\mathbf{r} \ll M$ most boxes are either mostly full or totally empty. As a result, the variance of box masses, and thus the lacunarity, is high over most of the range of box sizes. The slight initial increase of lacunarity as box size increases is due to the greater number of partially filled boxes at larger box sizes. Notice that once the box size reaches that of the clumps, the curve declines very rapidly.

In contrast, the points in set D are regularly distributed at a spacing of M/S. Once $\mathbf{r}$ is greater than this value, s would be constant at any location of the map, so the variance is zero. The lacunarity of a totally regular array is thus 1 for any gliding box size larger than the unit size of the repeating pattern. In addition, since the spacing of the points is M/S or $1/P$, the X and Y intercepts are identical and the slope of the lacunarity curve to this point should equal -1. The small deviations from zero for larger boxes shown in Fig. 2 are due to the length of the regularly spaced sequence being shorter than the total sampled length.

Sets B and C are intermediate cases. As expected, the lacunarity of the Lévy dust is higher over all box sizes than that of the random sequence, since the Lévy dust is hierarchically clumped. The lacunarity curve of the self-similar sequence is nearly linear. As described by Allain and Cloitre [7], the lacunarity curve for self-similar monofractals should be a straight line with a slope equal to $D-E$, where D and E are the fractal and Euclidean dimensions, respectively. The deviations from linearity in Fig. 2 are due to the short length of the sequence. Analyses of larger sets are much more linear [8]. Note also that, as expected, for the regular set D equals zero (D-$E=-1$) for box sizes smaller than the repeating pattern (each box contains only a single point).

The random set, in contrast, forms a concave upward curve, with a sharp dropoff at small box sizes. This is due to random patterns being statistically invariant at larger scales.

An examination of the lacunarity curve for set E, the randomly distributed clumps, demonstrates how lacunarity can be used to detect scales. The curve declines gradually to a break point at a log box size of about 0.6 (box size equal to 4), corresponding to the size of the clumps. It then declines more rapidly, with the concave upwards portion of the curve corresponding to the scales above that of random behavior.

In sum, lacunarity curves of one-dimensional sets have distinct breaks in slope corresponding to distinct scales within the sets. Fractal patterns, because they have the same appearance at all scales, produce straight lacunarity plots. This result is also true for higher dimensions [7,8].

B. An empirical example: γ-ray peaks from geologic well logs

Well logs of γ-ray emissivity versus depth are a standard technique for the measurement of the natural levels of radioactivity in rock formations. γ rays are predominantly emitted by ^{40}K, which is found in high concentration in clay-rich rocks, such as shales. Rocks with a low percentage of clays, such as clean sandstones, generally have a low level of radioactivity. Consequently, γ-ray well logs can be used to determine the vertical distribution of sand and shales in buried rock formations. Figure 3(a) shows the depth distribution of γ-ray emission peaks (''kicks'') in a portion of a well log from the Triassic Taylorsville basin of North Carolina. The rocks represent a long series of river-deposited sediments. The lacunarity curve for the entire sequence (831 peaks in 3439 feet) is shown in Fig. 3(b). For comparison, the lacunarity curve for the same number of randomly distributed peaks is also shown. It can readily be seen that the γ-ray peaks are far more clustered, at all scales, than would be predicted from a random distribution and more closely approximate a fractal distribution. This result is consistent with other studies that have shown the fractal structure of stratigraphic sequences [9,10].

C. Modifications for analysis of quantitative data

In many real data sets, the finest available resolution is greater than the grain of the data (i.e., the scale at which the data would resolve to point presence or absence). Such data are quantitative, rather than binary. Lacunarity analysis as originally applied [6,7] was used only on binary data sets. Further inspection of the method, however, reveals it is equally applicable to quantitative data. The box masses are 0's and 1's only for $r=1$. For all larger values of r, however, box masses can range from 0 to r in the one-dimensional case or 0 to r^2 in two dimensions (and so on for higher dimensions). Consequently, using quantitative data is analogous to beginning the analysis at a coarser level of resolution. The lacunarity can thus be calculated by using the sum (or integral) of the distribution in a box of size r.

In addition, recall that lacunarity is also a measure of the variance to mean ratio of box mass. In this context, if the total mass (or measure, *sensu* Mandelbrot [4]) is spread

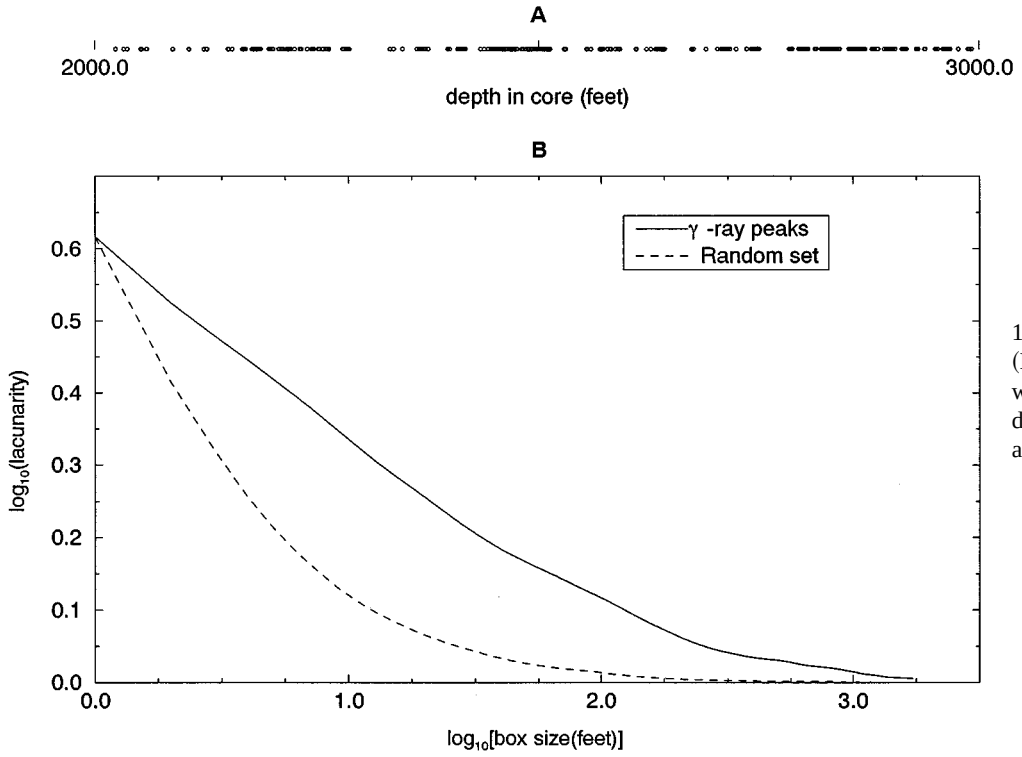

FIG. 3. (A) γ-ray peaks in 1000 foot section of a well log. (B) Lacunarity analysis of the well log peaks compared to a random distribution of the same overall density.

evenly over the entire set, then the variance, and thus the lacunarity, will be low. If the mass is concentrated at a few points, however, box mass variance and lacunarity will be high.

The application of lacunarity analysis to quantitative data can be illustrated by performing lacunarity analysis on a familiar multifractal set, that produced by the binomial multiplicative process [11]. The binomial multifractal can be used as a model of sequences where the distribution of material is produced by processes acting multiplicatively at many scales. Briefly, a given mass is distributed along a particular geometric support, such as a line. A fraction p of the mass is

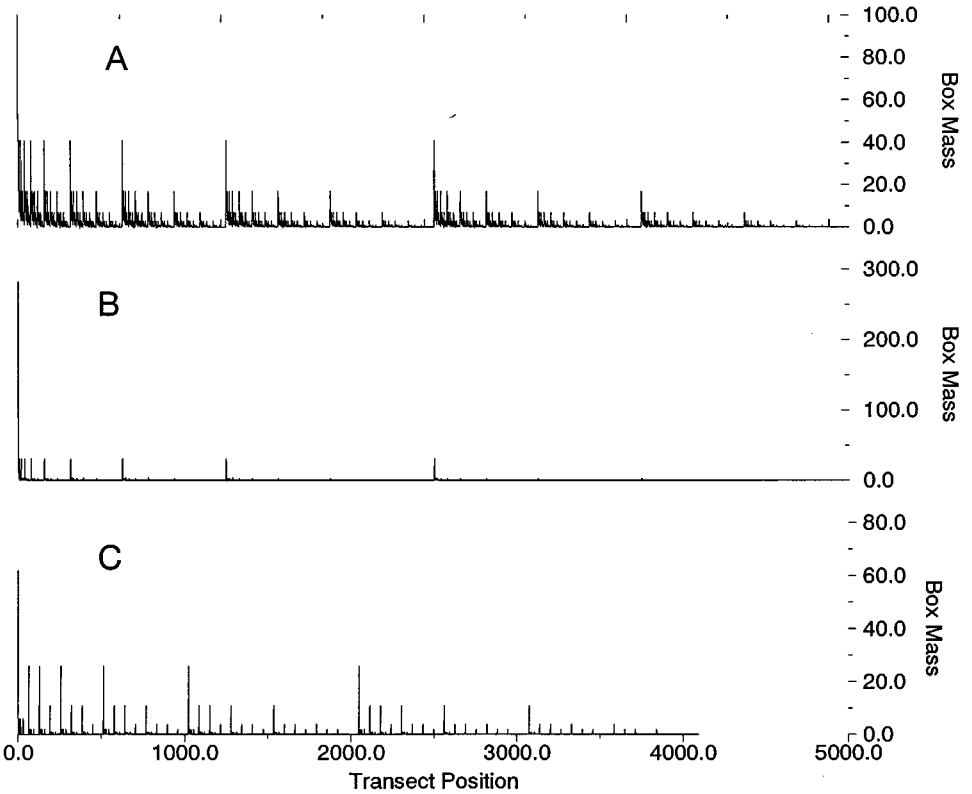

FIG. 4. (A) Results of an 11 generation binomial multiplicative process with $p=0.3$. (B) Same, $p=0.1$. (C) Process in which generations 1–6 have $p=0.1$ and generations 7–11 have $p=0.3$. Values on both axes are arbitrary.

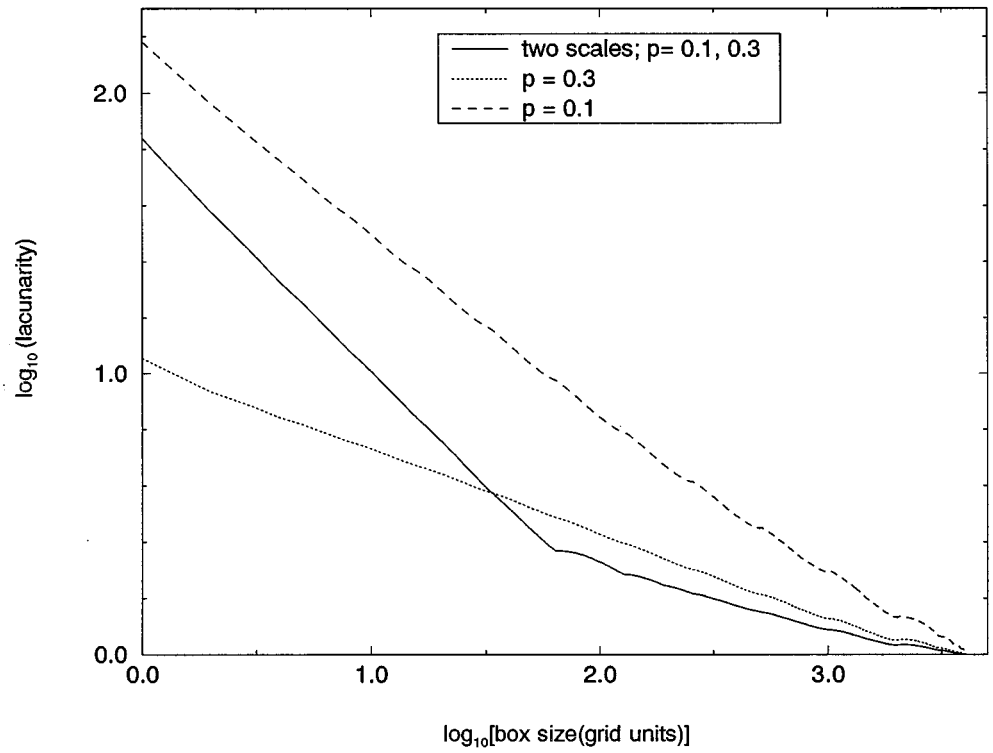

FIG. 5. Lacunarity analyses of the patterns shown in Fig. 4.

found on half the line, and a fraction 1-p along the other half. Each half line is also divided in half, with the same proportions of the material being found on each side. This procedure produces a self-similar distribution of masses, with some locations having extremely high values and others extremely low values. The range is a function of p. Two representative sets are shown in Figs. 4(a) and 4(b), with $p=0.3$ and 0.1, respectively. Notice that the lower the p value, the larger the range of masses after the same number of iterations.

The lacunarity curves for these distributions are shown in Fig. 5. As is the case for the fractals, the self-similar multifractals produce a linear lacunarity curve. Lacunarity can thus be used as a method to detect the presence of multifractal structure in a data set. The line for the $p=0.1$ has a higher intercept than that for $p=0.3$, reflecting the greater range of values in the latter sequence. Since the x intercept is fixed, the slope is also a function of p. Note that for these sets, the slope of the curve no longer represents the fractal dimension, as it does for monofractals.

As with fractals, lacunarity can be used to identify changes of scale within multifractal distributions. A two-scale binomial multifractal is shown in Fig. 4(c). The first six iterations were performed with $p=0.1$, the next five with $p=0.3$. The resulting lacunarity curve is shown in Fig. 5. Notice that the curve is more-or-less parallel to the line for $p=0.1$, up to a box size of 64, and then parallels the line for $p=0.3$. The break in slope thus corresponds exactly to the change in scaling of the original distribution. This immediately indicates how multifractal models can be compared to empirical data sets for the detection of scale-dependent changes in spatial behavior.

It may seem surprising that lacunarity analysis can be applied to multifractal distributions, since Mandelbrot [4], in his original formulation of the multifractal concept, referred to them as ''nonlacunar fractals.'' Future work should examine the relationship of lacunarity to other statistical representations of multifractals, such as $f(\alpha)$ curves and the distribution of mass exponents [11].

D. Examples: Yellowstone seedlings and sediment transport

The utility of lacunarity analysis as a general tool for spatial analysis of quantitative data is illustrated by its application to two diverse and seemingly unrelated data sets. The first data set, illustrated in Fig. 6, details the pattern of lodgepole pine seedling regrowth four years after the Yellowstone fires of 1988. The data were collected 23 July 1992 near Cougar Creek, just inside the Yellowstone National Park western boundary. The sequence represents the number of seedlings in consecutive 1 m^2 squares along a 3.4 km transect. Since the seedlings are very small, their distribution could be represented as binary only at a scale far smaller than that dictated by the sampling design.

The second data set (Fig. 7) is time series data of bedload transport rates (mass of sediment passing a particular point per unit time) in the East Rosebud River, Montana, in July 1988. Bedload transport rate was measured at 1 min intervals for 10 h [9].

Both of the empirical distributions are probably produced by interacting multiplicative processes acting at many scales (see below). As a result, comparison sequences were generated by modifying the binomial multiplicative process (Fig. 8). Instead of the left (or right) side of the segment always receiving the same proportion of material at each iteration, the side receiving the largest fraction was randomly chosen. As a result, the peaks are generally symmetrical. In addition,

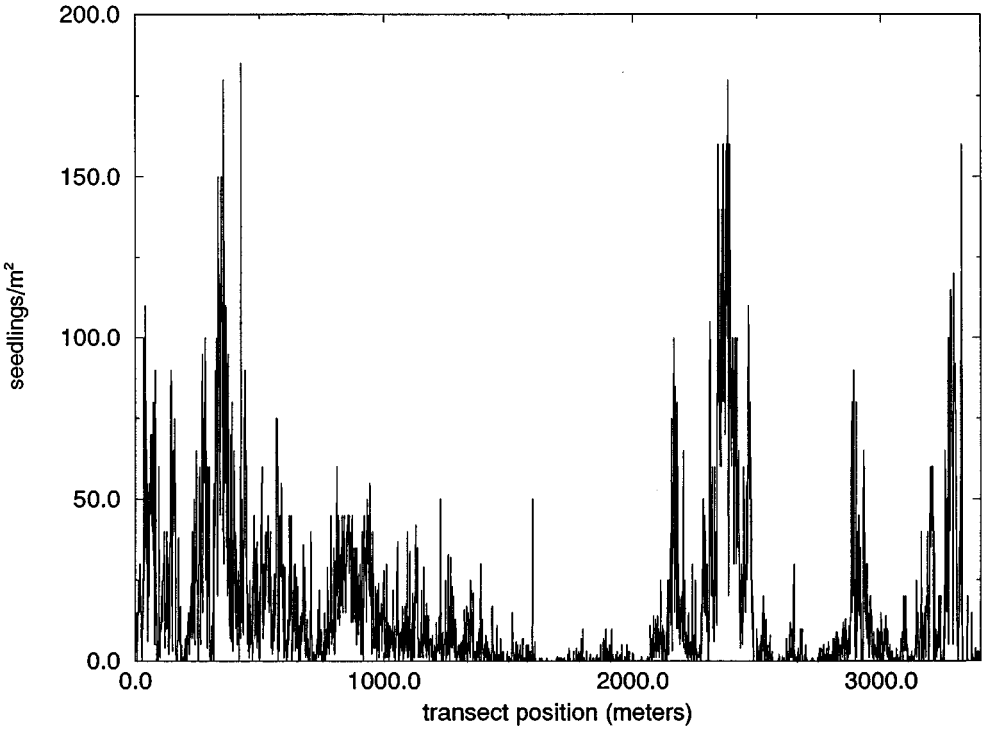

FIG. 6. Number of lodgepole pine seedlings per m^2 in a 3.4 km transect, Yellowstone National Park.

the exact proportions are allowed to vary normally around the mean value of $p=0.4$. The sequence produced is much closer in appearance to the empirical data sets shown in Figs. 6 and 7 than are the binomial sequences in Fig. 4.

The lacunarity curves for these sequences are shown in Fig. 9. In order to facilitate comparisons, the curves were normalized to a common y intercept by dividing through by the value for box size equal to 1.

Note first that despite the randomization, the random multifractal sequences produce an essentially linear lacunarity curve. In contrast, both curves for the empirical data show distinct breaks in slope. These breaks may represent scale-related changes in the dominant process controlling the distribution.

For example, the Yellowstone curve is linear to a box size of about 25 m, a distance approximately equal to the distribution of seedlings around individual isolated parent trees. Other changes in slope may reflect variations in the effects of topography, soil suitability, and fire severity. An important biological factor may be spatial variation in the distribution

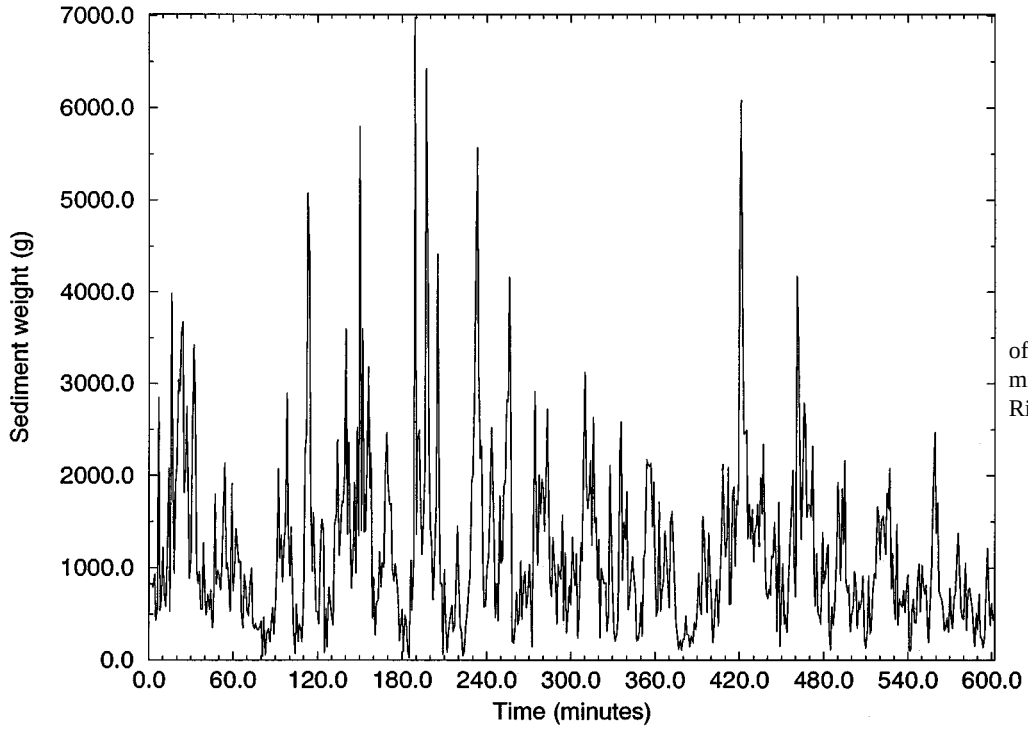

FIG. 7. Time series of weight of sediment in transport per minute for 10 h, East Rosebud River, Montana [9].

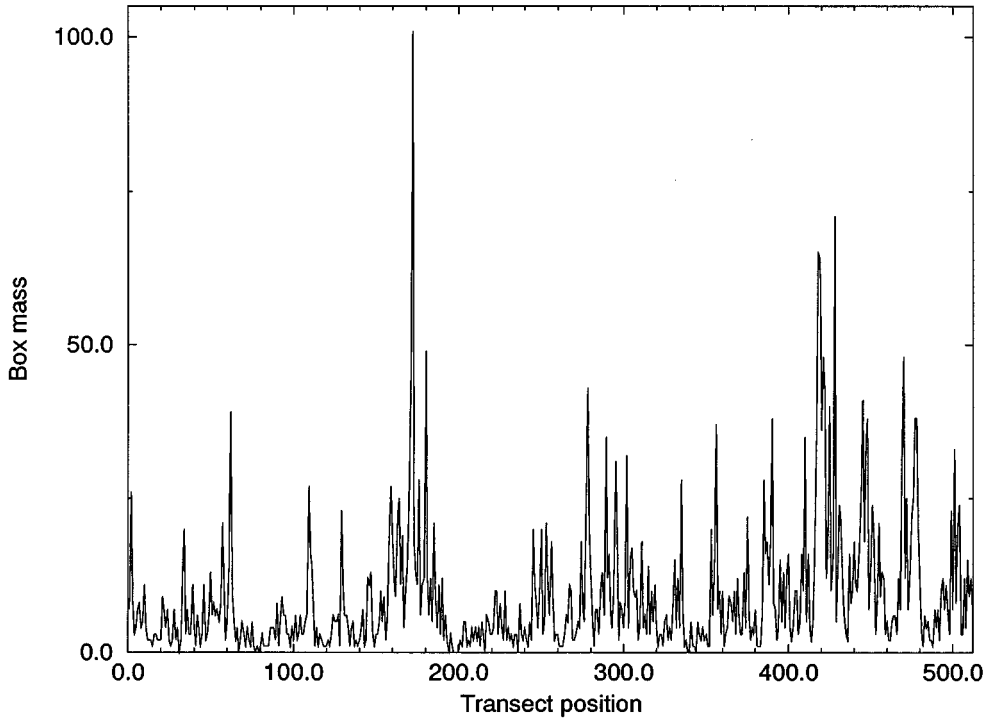

FIG. 8. Randomized binomial multiplicative process, with p approximately 0.4. Values on both axes are arbitrary.

of serotiny, a trait present in some lodgepole pines, in which fire is required to open the pine cones and thus distribute seeds. These physical and biological factors all act at specific scales.

Similarly, the sediment transport curve shows distinct breaks at about 4 and 30 min. These changes in behavior may result from nonlinear feedbacks between the heterogeneous material on the stream bed, the material in transport, and local fluctuations in stream hydraulics [12].

III. DISCUSSION

Although fractal methods are starting to become part of the standard approach to the analysis of spatial patterns, they are often inadequate to describe the full range of real patterns. Real patterns may or may not be fractal; when fractal structure exists, it may be only over a limited range of orders of magnitude; and patterns with the same fractal dimension may still look different; i.e., have different ''textures'' [4].

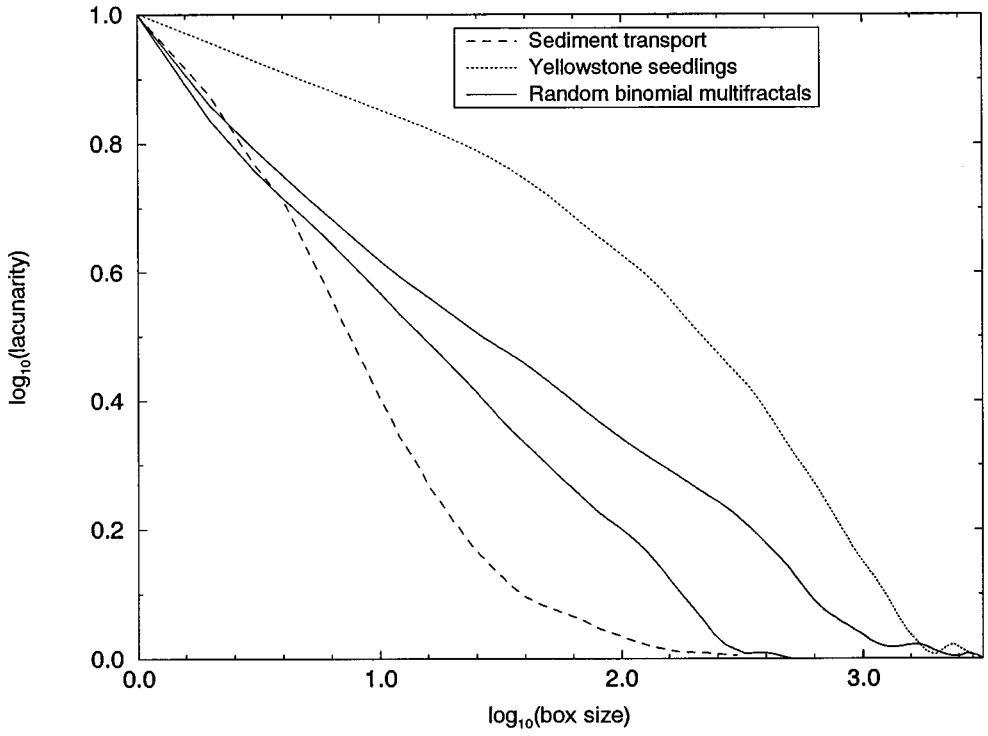

FIG. 9. Lacunarity analysis of the patterns in Figs. 6 and 7, compared to similar length randomized binomial multiplicative processes.

Lacunarity analysis, in contrast, is a far more general technique. It can be applied to data of any dimensionality, to both binary and quantitative data, and to fractal, multifractal, and nonfractal patterns. It allows the determination of scale-dependent changes in spatial structure, which should give insight into underlying processes. Lacunarity analysis also reveals the presence and range of self-similarity. The technique is easily implemented and gives readily interpretable graphic results. We believe it will find wide applicability in those fields concerned with description of spatial patterns; in fact, it has already been successfully applied in the analysis of synthetic aperture radar imagery [13].

ACKNOWLEDGMENTS

Texaco, Inc. is thanked for providing the well log data. Research was funded by the Ecological Research Division, Office of Health and Environmental Research, U.S. Department of Energy under Contract No. DE-AC05084OR21400, and by grants from the National Science Foundation to R.E.P. and K.P. (Grant No. EAR-890484) and to W. Romme, M. Turner, and R.H.G. (Grant No. BSR-901831), and from Texaco, Inc. to R.E.P. Parts of this work appeared in different form in [14].

[1] *Fractals in Petroleum Geology and Earth Processes*, edited by C. C. Barton and P. R. La Pointe (Plenum, New York, 1995).

[2] B. Milne, in *Quantitative Methods in Landscape Ecology*, edited by M. G. Turner and R. H. Gardner (Springer-Verlag, New York, 1991).

[3] *Fractals in Geography*, edited by N. S. Lam and L. De Cola (Prentice-Hall, Englewood Cliffs, N.J., 1993).

[4] B. Mandelbrot, *The Fractal Geometry of Nature* (Freeman, New York, 1983).

[5] B. Lin and Z. R. Yang, J. Phys. A **19**, L49 (1986).

[6] Y. Gefen, Y. Meir, and A. Aharony, Phys. Rev. Lett. **50**, 145 (1983).

[7] C. Allain and M. Cloitre, Phys. Rev. A **44**, 3552 (1991).

[8] R. Plotnick, R. H. Gardner, and R. V. O'Neill, Landscape Ecology **8**, 201 (1993).

[9] R. Plotnick and K. Prestegaard, in *Fractals in Petroleum Geology and Earth Processes*, edited by C. C. Barton and P. R. La Pointe (Plenum, New York, 1995).

[10] G. Korvin, *Fractal Models in the Earth Sciences* (Elsevier, Amsterdam, 1992).

[11] J. Feder, *Fractals* (Plenum, New York, 1988).

[12] K. Prestegaard and R. Plotnick, in *Fractals in Petroleum Geology and Earth Processes*, edited by C. C. Barton and P. R. La Pointe (Plenum, New York, 1995).

[13] G. M. Henebry and H. J. H. Kux, Int. J. Remote Sensing **16**, 565 (1995).

[14] R. Plotnick, in *Nonlinear Dynamics and Fractals: New Numerical Techniques for Sedimentary Data. SEPM Short Course No. 36*, edited by G. V. Middleton, R. Plotnick, and D. M. Rubin (SEPM: Society for Sedimentary Geology, Tulsa, 1995).